Journal of Information Hiding and Multimedia Signal Processing ©2011 ISSN 2073-4212
Ubiquitous International Volume **2**, Number **4**, October **2011**

Statistical Measurement of Ultrasound Placenta Images Complicated by Gestational Diabetes Mellitus Using Segmentation Approach

G. Malathi

Assistant Professor, Department of Computer Applications
Velammal Engineering College, Chennai
malathirajsuresh@gmail.com

Dr. V. Shanthi

Professor, Department of Computer Applications
St.Josephs Engineering College, Chennai
drvshanthi@yahoo.com.in

Received April 2010; revised November 2010

Abstract. *Medical diagnosis is the major challenge faced by the medical experts. Highly specialized tools are necessary to assist the experts in diagnosing the diseases. Gestational Diabetes Mellitus is a condition in pregnant women which increases the blood sugar levels. It complicates the pregnancy by affecting the placental growth. The ultrasound screening of placenta in the initial stages of gestation helps to identify the complication induced by GDM on the placental development which accounts for the fetal growth. This work focus on the classification of ultrasound placenta images into normal and abnormal images based on statistical measurements. The ultrasound images are usually low in resolution which may lead to loss of characteristic features of the ultrasound images. The placenta images obtained in an ultrasound examination is stereo mapped to reconstruct the placenta structure from the ultrasound images. The dimensionality reduction is done on stereo mapped placenta images using wavelet decomposition. The ultrasound placenta image is segmented using watershed approach to obtain the statistical measurements of the stereo mapped placenta images. Using the statistical measurements, the ultrasound placenta images are then classified as normal and abnormal using Back Propagation neural networks.*

Keywords: Placenta, Gestational Diabetes Mellitus, Segmentation, Wavelet, Stereo Mapping, Classification, Watershed Algorithm

1. **Introduction.** The Placenta is the organ within the uterus by means of which the embryo is attached to the wall of the uterus. Its main function is to provide the embryo with nourishment, eliminate its wasters, and exchange respiratory gases. This is accomplished by the close proximity of the maternal and fetal blood systems within the placenta [1]. An ultrasound exam is a procedure that uses high-frequency sound waves to scan and create a 2D picture [2] of the area of interest. Gestational diabetes is much more common than pre-existing diabetes i.e. it complicates 2% to 5% of pregnancies. There is change of shape i.e. two lobes in one placenta from diabetic group. All other placenta was singly lobed and discoid shape with central attachment of umbilical cord to the fetal surface of placenta. Weight central thickness and diameter were significantly greater in diabetic group as compared to normal and hypertensive group. Hypertensive group shows non

significant decrease in weight of placenta while there was no change in central thickness and diameter of placenta in hypertensive than the normal group. it is concluded that diabetic's placenta showed increase in weight, central thickness and diameter[3].

In [4], the classification of ultrasonic images of the placenta according with the gradation proposed by Grannum is attempted. The ability of the decision tree classifier to discriminate different textures with three sets of textural features was tested. The performance of the classifier using textural features corresponding to co-occurrence matrices, Laws operators and neighborhood gray-tone difference matrices applied to the classification of ultrasonic images of the placenta corresponding to different grades. In [5] an attempt to classify the scans of placenta according with Grannum grading using feature selection for determining the relevant textural features from the scans was made.

The study carried out in [6] concluded that the diabetics placenta showed increase in weight, central thickness and diameter while there are no change in central thickness and diameter of placenta in hypertensive than the normal group. In a previous work [7], a pilot study was carried out to find the feasibility for detecting anomalies in placental growth due to the implications of gestational diabetes by considering the stereo image mapping based on wavelet analysis for 2D reconstruction. The research used wavelet-based methods to extract features from the ultrasonic images of placenta. Euclidean Distance Classifier is used for classifying the ultrasonic images of placenta. In a recent work [8], the authors have made an attempt to classify the placenta based on the intensity level of histogram of the ultrasound images of placenta. The image histogram is used to classify the ultrasound images of placenta into normal and abnormal placenta using k nearest neighbor classifier to analyze the complications of gestational diabetes mellitus on the growth of the placenta. The pilot study [19] involves the feasibility for classifying the ultrasound images of placenta with complicating diabetes based on placenta thickness using statistical textural features.

2. **Stereo Image Mapping.** Stereo Image Mapping is a technique for creating a 3D or 2D description of a scene observed from several view points. Usually two cameras are used to observe the same scene from two slightly different view points and the stereo image pairs are obtained. After that the left image and right image in the stereo image pair are matched. It plays an important part in 2D description. The ultrasonic images obtained are low in resolution. The placenta is a curved structure and so becomes difficult to measure accurately. The resolution is improved by combining the features of the placenta image obtained by the left focus and the placenta image obtained by the right focus. This stereo mapping reveals the important features of the placenta images obtained by ultrasound.

3. **Wavelet Decomposition of an Image.** Wavelets are functions generated from one single function by transformations like dilations and translations. Decomposition of the given image into different levels where each levels is further decomposed with a resolution adapted to that level is called Wavelet Decomposition. The values of the transformed coefficients are the essential features which are useful for texture classification and segmentation. These are the features that uniquely characterize a texture. Normally the ultrasound images are low in resolution. The critical information is lost. The wavelet decomposition of the ultrasound retains the essential features. The classification accuracy also increased when the ultrasound images are wavelet decomposed and stereo mapped. The ultrasound images of placenta are first decomposed using Haar wavelet into five levels. The figure 5 and figure 6 shows the five level decomposition of the left focus ultrasound placenta and right focus ultrasound placenta images.

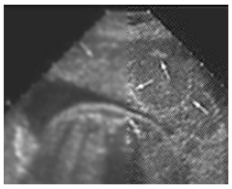

FIGURE 1. Left Placenta Image

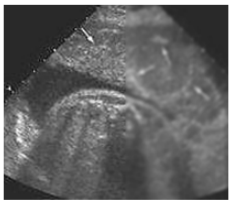

FIGURE 2. Right Placenta Image

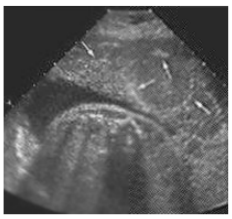

FIGURE 3. Stereo Mapped Placenta Image

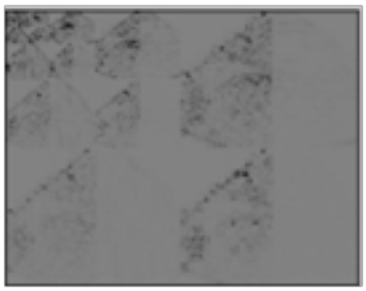

FIGURE 4. Decomposition of left Placenta.

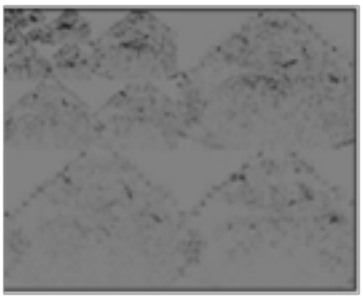

FIGURE 5. Decomposition of right Placenta.

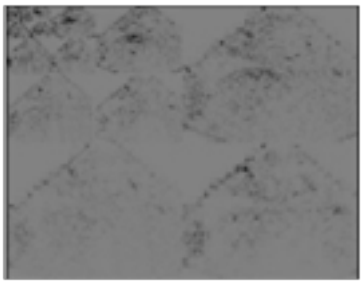

FIGURE 6. Fusion of decomposed images.

4. **Modalities.** Segmentation methods have been applied to various medical imaging modalities.

4.1. **Magnetic resonance imaging.** The major application of medical image segmentation is brain imaging. The MRI images provides a combination of high resolution. It provides excellent soft tissue contrast and a high signal-to-noise ratio.

4.2. **Chest radiography.** The application of segmentation is less in chest radiographs because the nature of the image makes quantification and localization a difficult task. The Markov random field and classifiers were used for segmenting chest radio graphs into anatomical regions.

4.3. **Computed tomography.** X-ray computed tomography was mainly used for imaging bone and bone tumors. The soft tissue contrast is comparatively less than MRI.. Statistical clustering has been used to segment thoracic scans and a combination of region growing and watershed algorithms have been used in brain segmentation of CT images.

4.4. **Digital mammography.** In digital mammography segmentation is used for localization of tumors and micro calcification clusters. Thresholding and its variations are the frequently used segmentation techniques in mammography.

4.5. **Ultrasound. Segmentation algorithms have a limited application in ultrasound image.** The presence of high levels of speckling in ultrasound images makes accurate segmentation difficult. The region of interest is typically obtained through manual interaction. Deformable models were used to determine the boundary of the fetus and its head, segment cysts in breast images, segmentation of pubic arch in transrectal ultrasound[11]. Thresholding of intensity and texture statistics was used to segment ovarian cysts.

5. **Image Segmentation.** Segmentation is carried out by comparing co-occurrence matrix features. Contrast and Energy of size N x N derived from discrete wavelet transform overlapping but adjacent sub images Ci,j of size 4 x 4, both horizontally and vertically[21]. The common image segmentation techniques are thresholding, edge-based segmentation, mean shift segmentation, watershed segmentation.

5.1. **Thresholding.** In thresholding all the pixels brighter specific brightness level are taken as 1 and all the other taken as 0. The binary image is obtained with useful details represented as 1 and others represented as 0 [17]. Thresholding is the transformation of an input image to an output image g as follows:

$$G(i,j) = \begin{cases} 0, & f(i,j) \le T \\ 1, & f(i,j) \ge T, \end{cases} \tag{1}$$

where ,
$T = threshold$
$G(i,j) = 1$ for image elements of object
$G(i,j) = 0$ for image elements of background
thresholds are determined independently in each sub image and is then processed with respect to its local threshold.

5.2. **Edge Based Segmentation.** Edges occur on the boundary between two different regions in an image. The technique may be classified as derivative based on first or second order derivative on each pixel or gradient based where a gradient of consecutive pixels is taken in x and y direction. The edges identified by edge detection are often disconnected. The disconnected regions boundaries must be closed to generate segmented image[22]. The gradient magnitude includes sobel, prewitt, canny, laplacian, zero crossings and Roberts.

5.2.1. *Sobel Edge Detection.* The operator consists of a pair of 3 x 3 convolution kernels as shown in Figure 1. One kernel is simply the other rotated by 90° These kernels are designed to respond maximally to edges running vertically and horizontally relative to the pixel grid, one kernel for each of the two perpendicular orientations. The kernels can be applied separately to the input image, to produce separate measurements of the gradient component in each orientation Gx and Gy. These can then be combined together to find the absolute magnitude of the gradient at each point and the orientation of that gradient. The gradient magnitude is given by [10],[13]:

$$|G| = \sqrt{Gx^2 + Gy^2} \tag{2}$$

5.2.2. *Roberts Edge Detection.* It is used to compute the 2D spatial gradiant measurement of an image [10],[14]. It is similar to Sobel operator. The pixel values at every point in the output are the estimation of absolute magnitude of the spatial gradient. The gradient magnitude is given by equation(2).

5.2.3. *Prewitts Edge Detection.* The prewitts operator [10], [15] is used to estimate the magnitude and orientation of an edge which calculates the maximum response of a set of convolution kernels to find the local edge orientation for each pixel. The maximum response for each pixel is the value of the corresponding pixel in the output magnitude image. The values for the output orientation image lie between 1 and 8, depending on which of the 8 kernels produced the maximum response. The horizontal and vertical edges in an image can be detected. If I is the original image , the Gx and Gx are the horizontal and vertical derivative approximations then,

$$Gx = \begin{bmatrix} -1 & 0 & +1 \\ -1 & 0 & +1 \\ -1 & 0 & +1 \end{bmatrix} * I \quad Gy = \begin{bmatrix} -1 & -1 & -1 \\ 0 & 0 & 0 \\ +1 & +1 & +1 \end{bmatrix} * I \tag{3}$$

5.2.4. *Canny Edge Detection.* The canny edge detector first smoothes the image to eliminate and noise. It then finds the image gradient to highlight regions with high spatial derivatives. The algorithm then tracks along these regions and suppresses any pixel that is not at the maximum (no maximum suppression). The gradient array is now further reduced by hysteresis which is used to track along the remaining pixels that have not been suppressed. It uses two thresholds and if the magnitude is below the first threshold, it is set to zero (made a non edge). If the magnitude is above the high threshold, it is made an edge and if the magnitude is between the 2nd thresholds, then it is set to zero unless there is a path from this pixel to a pixel with a gradient above threshold two [10],[16].

Gaussian smoothing is performed using standard convolution methods. The edge strength is obtained by taking the gradient of the image. The edge strength is obtained by

$$|G| = |Gx| + |Gy| \tag{4}$$

$$|G| = \sqrt{Gx^2 + Gy^2} \tag{5}$$

Where G is the edge gradient , Gx is the first derivative in horizontal direction , Gy is the first derivative in vertical direction.
The edge direction is obtained by

$$\theta = \arctan(\mathrm{Gy}/\mathrm{Gx}) \tag{6}$$

5.2.5. *Laplacian of Gaussian.* Laplacian Edge detection searches for the zero crossing in the second derivative of the image [10],[12]. It highlights the regions of rapid change in intensity of the image. Let I = (x,y) be the intensity of the pixel at x,y. The laplacian L(x,y) of the pixel intensity I(x,y) is given by,

$$L(x, y) = d2l/dx2 + d2l/dy2 \tag{7}$$

5.3. **Mean Shift.** It is a data-clustering method that searches for the local maximal density points and then groups all the data to the clusters defined by these maximal density points. When used for image segmentation, each pixel xi, $i = 1, K, n$, in the image is treated as an input data, and the density at point x is estimated by,

$$f(x) = c/NH^D \sum_{n}^{1} K\left(\left\|\frac{x - xi}{h}\right\|\right)^2 \tag{8}$$

h is bandwidth , d refers to data dimensionality and K(-) refers to density estimation kernel [18].

5.4. **Region Growing.** Region growing is a technique for extracting a region of the image that is connected based on some predefined criteria. These criteria can be based on intensity information and/or edges in the image. A variation of region growing is seeded region growing which takes a set of seeds as input along with the image. The seeds mark each of the objects to be segmented. The regions are iteratively grown by comparing all unallocated neighboring pixels to the regions. The difference between a pixel's intensity value and the region's mean is used as a measure of similarity. The pixel with the smallest difference measured this way is allocated to the respective region. This process continues until all pixels are allocated to a region. In [20], an attempt was made to extract the feature of ultrasonic images of placenta using region growing method and classified the features using K nearest neighbor.

5.5. **Histogram based Segmentation.** A histogram is computed from all of the pixels in the image, and the peaks and valleys in the histogram are used to locate the clusters in the image.

5.6. **Watershed Segmentation using Distance Transform.** The distance transform is the common tool used together with the watershed transform. It represents the distance from each pixel with its value of 1 to the nearest nonzero-valued pixel. The original gray-scale image to binary image at first using optimal global image threshold. In the next step image complement is defined. Image transform using the watershed method should be applied to a matrix after its proper preprocessing to obtain the best image objects contours with results presented in figure 15. All zero pixels of the complementary image have been assigned by $-\infty$ at first. The matrix processed by the watershed transform in the next step resulted in a labeled matrix identifying the watershed regions with its integer elements greater than or equal to 0. Its zero values identify image contours and nonzero elements belong to watershed regions. The final operation consists of the assignment of values 1 to zero elements and values 0 to all nonzero elements with results presented in figure 13.

5.7. **Comparison of Edge Based Segmentation Methods.** Edge detection was performed on the synthesized image with Sobel, Prewitt, Canny, Laplacian of Gaussian, Roberts and Watershed. The ultrasound placenta image, which is synthesized as a result of wavelet decomposition stereo mapping, gives closer to accurate results when compared

to classification done with the original ultrasound placenta. It is found that the watershed segmentation of synthesized ultrasound placenta provides better segmentation when compared to other edge based segmentation methods. The results of segmentation follows:

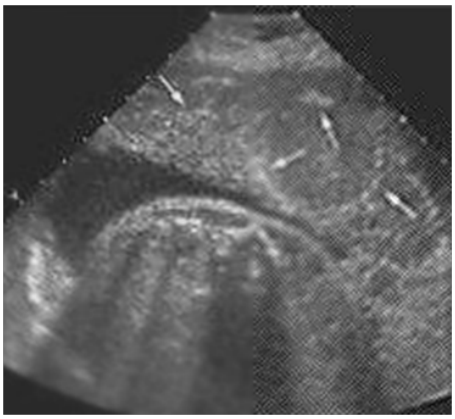

FIGURE 7. Synthesized Image.

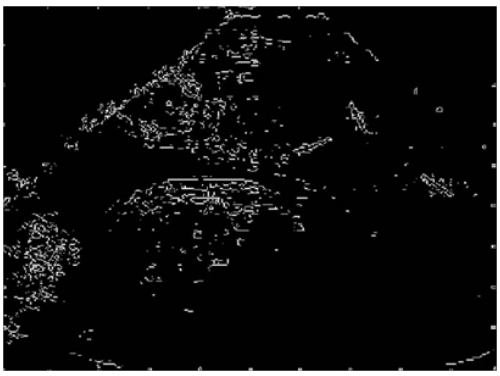

FIGURE 8. Sobel.

FIGURE 9. Laplacian of Gaussian.

FIGURE 10. Canny.

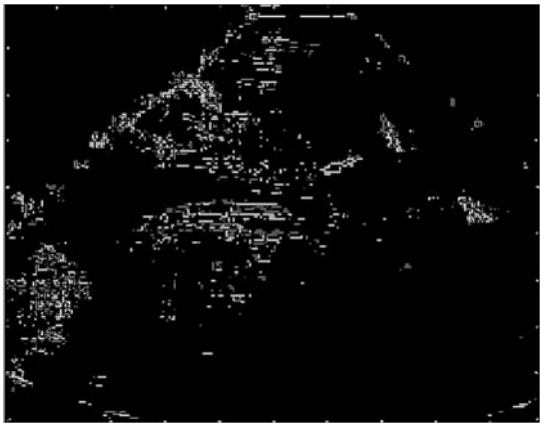

FIGURE 11. Roberts.

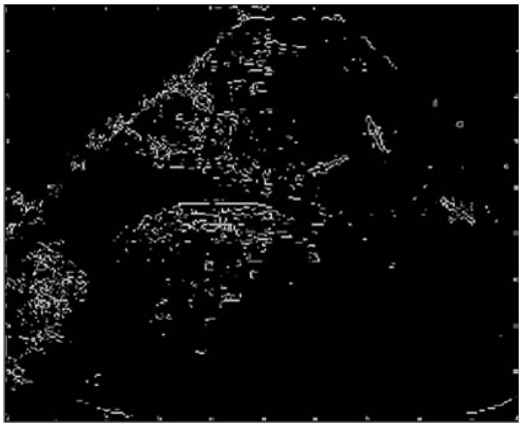

FIGURE 12. Prewitt.

FIGURE 13. Watershed Markers and object boundaries superimposed on original image.

FIGURE 14. Segmented Bina-ry Image.

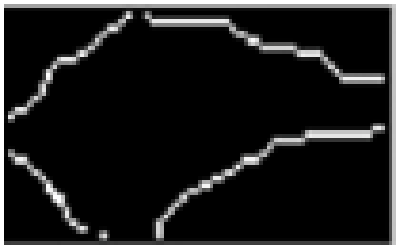

FIGURE 15. Contour Extracted Image.

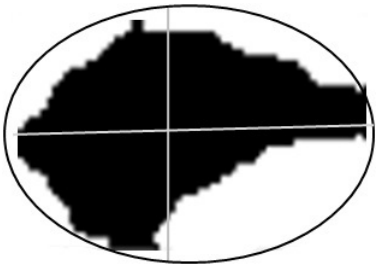

FIGURE 16. Measurement of Major axis length and Minor axis length to calculate area and perimeter.

Figure 14 represents the segmented ultrasound placenta images. Statistical measurements of this segmented ultrasound placenta images are generated by measuring the major axis length and minor axis length which is shown in figure 16.

In a previous work [8] , the author has obtained the Haralick features[11] for ultrasound placenta images. The results are shown in Table1. Based on the threshold values the images were classified into normal and abnormal placenta. The abnormal placenta is further classified into abnormal condition due to implications of diabetes mellitus and abnormal condition due to other complications. A study [6] revealed that the mean diameter of placenta is significantly more in the case of gestational diabetes group. In this paper, area and perimeter of the segmented placenta are obtained to support the classification of ultrasound placenta images into normal and abnormal images. It was then compared with the opinion of the medical experts. The figure 17 shows the ultrasonic measurement of placental thickness [9].

$p(i,j)$ is the (i,j) th entry in a normalized gray-tone spatial dependence matrix. The gray level cooccurrence matrix is given by

$$P_{d,r}(i,j) = \frac{P(i,j)}{R} \tag{9}$$

FIGURE 17. Measurement of Placental thickness.

Mean. It returns the mean values of the elements along different dimensions of an array. It is the measure of homogeneity of the image.

$$Px(i) = \sum_{j=1}^{Ng} P(i,j) \tag{10}$$

$$Py(j) = \sum_{j=1}^{Ng} P(i,j) \tag{11}$$

Contrast. It creates a new gray colormap that has an approximately equal intensity distribution. It is a difference momentum of the matrix and is a measure of the contrast or the amount of local variations present in an image. Table 1 shows that the contrast of abnormal placenta image is higher than the normal image.

$$\sum_{n=0}^{Ng-1} n2 \left\{ \sum_{i=1}^{Ng} \sum_{j=1}^{Ng} p(i,j) \right. \tag{12}$$

Ng is the number of distinct gray levels in the quantised image
Correlation. It is a measure of gray-tone linear-dependencies in the image. The correlation features of abnormal placenta images is higher than the normal placenta image which is mentioned in Table 1.

$$\frac{\sum_i \sum_j (i,j) p(i,j) - \mu x \mu y}{\sigma x \sigma y} \tag{13}$$

Where gx and gy is the mean mx and my is the standard deviation or the measure of contrast
Entropy. It is a statistical measure of randomness that can be used to characterize the texture of the input image

$$-\sum_i \sum_j p(i,j) \log(p(i,j)) \quad \sum_i \sum_j (i-\mu) 2p(i,j) \tag{14}$$

Sum of Squares. It is the measure of variation within a data set. It is used in calculating the standard deviation, which is a scaled method of comparing variance between data sets.

$$\sum_i \sum_j (i-\mu) 2p(i,j) \tag{15}$$

Table 1 shows the measure of Mean, Contrast, Correlation, Entropy and Sum of Squares which plays an important role in the classification of placenta into normal and abnormal.

Maternal diabetes is a condition associated with large placentas. Large placentas should raise the suspicion of large placentas [9]. In Table 2, Class AN(GDM) refers to Abnormal Placenta due to the complications of Gestational Diabetes Mellitus, AN refers to the Abnormal Placenta due to other complications. The Class N refers to the normal healthy placenta without any complications. The Table 2 shows the statistical measurement of

TABLE 1. Haralick Features for Ultrasound Placenta Images for sample images

Images	Mean	Contrast	Correlation	Entropy	Sum of squares	Class
Image1	1.635 e4	1310473767	7.922339e5	8.944150e4	7.2	AN
Image2	1.832 e4	1614852030	2.978678e6	1.047565e5	1.1	AN
Image3	1.454 e4	1434646325	1.911394e5	9.609855e4	5.6	AN(GDM)
Image4	1.455 e4	1436691775	1.915322e5	9.670916e4	1.0	AN
Image5	1.222 e4	1077321331	1.055089e5	7.347292e4	1.2	N
Image6	1.832 e4	1614852030	2.978678e6	1.047565e5	2.5	AN
Image7	1.854 e4	1647605895	9.059511e5	7.575653e4	1.7	AN
Image8	1.749 e4	1531849951	7.756140e5	9.824614e4	2.15	AN
Image9	1.263 e4	1083142018	1.065980e5	9.824614e4	1.2	N
Image10	1.280 e4	1067278301	1.065980e5	7.367722e4	1.14	N

TABLE 2. Statistical Measurement Area, Perimeter of Segmented Image for sample images

Images	Area	Perimetert	Class
Image1	3.2167	6.7019	AN
Image2	6.00154	11.7823	AN
Image3	10.2083	14.8600	AN(GDM)
Image4	6.8913	9.9025	AN
Image5	7.3428	10.3109	N

area and perimeter of the segmented image. The results shows a significant increase in area and perimeter when compared to normal placenta findings (Image5) and abnormal placenta due to other complications (Image1,Image2,Image4) and abnormality due to complications of gestational diabetes mellitus (Image3).

6. **Work Flow.**

Input rightfocus image1
Input leftfocus image2

1.Let D=Image Database which consist of placenta images pairs with left focus and right focus im-
ages
for I=0 to image.height **do**
for For J=0 to image.width **do**
Temp=Max((leftfocusimage1(I,J),rightfocus image1(I,J))
end for
end for
2.Call WaveFeature Refer[7]
3.Apply WaterShed(WaveFeature)
4.For each WaterShed Image
Compute,
Mean = Eq 10 & Eq 11
Contrast= Eq 12
Correlation = Eq 13
Entropy = Eq 14

```
    Sum of squares = Eq 15
  Area = [m,n]= size(A)
for i= 1:m do
  for j= 1:n do
    if (A (i,j)== 1) then
      increment A counter
    end if
  end for
end for
5.Perimeter = [m,n]= size(B);
6.
for i=1:m do
  for j=1:n do
    if (B(i,j)==1) then
      Increment PR counter
    end if
  end for
end for
7. P= 0.126;
8. Area= A * P^2;
9. Perimeter=PR * P;
```

7. **Conclusions.** The work carried out showed that the statistical measurements along with the image, textural features are suitable for the classification of ultrasound placenta images. The best results were obtained when wavelet decomposed and stereo mapped ultrasound placenta images were used for segmentation. This reduces the chance of misclassication of abnormal placenta being classified as normal. The work can be extended by developing technique to project this segmented image in an 3D visualization for volumetric analysis.

Acknowledgment. The authors gratefully acknowledge the helpful comments and suggestions of the reviewers, which have improved the work.

REFERENCES

[1] Oxford, *Concise Medical Dictionary*, Oxford University Press, Market House Hooks Ltd, 1998.
[2] Cunningham, F. Gary, et. al, Williams Obstetrics Twenty-Second Ed, American Pregnancy Association, http://www.americanpregnancy.org/prenataltesting/ultrasound.html
[3] M. Ashfaq, M. Z. Janjua, M. A. Channa, Effect of gestational diabetes and maternal hypertension on gross morphology of placenta, *Journal of Ayub Medical College*, vol. 17, no.1, pp. 44-7, 2005.
[4] P. A. Linares, P. J. McCullagh, N. D. Black, J. Dornan, Characterization of ultrasonic images of the placenta based on textural features, *Proc. of the 4th Annual IEEE Conference on Information Technology Applications in Biomedicine*, UK, pp. 211-214, 2003.
[5] P. A. Linares, P. J. McCullagh, N. D. Black, J. Dornan, Feature Selection for the characterization of ultrasonic images of the placenta using texture classification, 2004.
[6] M. Ashfaq, M. Zahoor, Janjua, and M. A. Channa, Effect of gestational diabetes and maternal hypertension on gross morphology of placenta, www.ayubmed.edu.pk/.JAMC/PAST/17-1/Ashfaq.htm
[7] G. Malathi, Dr. V. Shanthi, Wavelet based features for ultrasound placenta images classification, *Proc. of the 2nd International Conference on Emerging Trends in Engineering and Technology*, Nagpur, pp. 341-345, 2009.
[8] G. Malathi, Dr. V. Shanthi, histogram based classification of ultrasound images of placenta, *International Journal of Computer Applications*, http://www.ijcaonline.org/arc-hives/number16/343-522, 2010.

[9] Lois Jovanovic, Gian Carlo Di Renzo, Alberto De Leiva, Oded Langer, Textbook of Diabetes and Pregnancy, Second Edition, *Series in Maternal-Fetal Medicine-Edited by Moshe Hod*, Amazon, 2003.
[10] T. Moravcik, *Image Segmentation in Programming Environment MATLAB*, XI International Ph. D Workshop, University of Zilina, Poland, 2009.
[11] R. M. Haralick and L. G. Shapiro, Image segmentation techniques, *Proc. of Computer Vision, Graphics*, vol. 29, pp. 100-132, 1985.
[12] F. Bergholm, Edge focusing, *Proc. of the 8th International Conference Pattern Recognition*, Paris, France, pp. 597-600, 1986.
[13] J. Matthews, An introduction to edge detection: The sobel edge detector, Available at http://www.generation5.org/content/2002/im01.asp, 2002.
[14] L. G. Roberts, Machine perception of 3-D solids, *Optical and Electro-optical Information Processing*, MIT Press, 1965.
[15] R. C. Gonzalez and R. E. Woods, *Digital Image Processing*, 2nd Edition, Prentice Hall, 2002.
[16] J. F. Canny, A computational approach to edge detection, *IEEE Trans. Pattern Analysis Machine Intelligence*, vol. PAMI-8, no. 6, pp. 679-697, 1986.
[17] M. Sonka, V. Hlavac, and R. Boyle, *Image Processing, Analysis and Machine Vision*, Third Edition, Thomson, 2008.
[18] Dr. S. V. Kasmir Raja, A. Shaik Abdul Khadir, Dr. S. Riaz Ahamed, Moving toward region-based image segmentation techniques: A study, *Journal of Theoretical and Applied Information Technology*, 2005-2009.
[19] G. Malathi, Dr. V. Shanthi, Thickness Based Characterization of Ultrasound Placenta Images Using regression analysis, *International Journal of Computer Applications*, vol. 3, no. 7, pp. 7-11, 2010,
[20] G. Malathi, Dr. V. Shanthi, Classification of ultrasonic images of placenta based on seeded region growing approach, *International Journal on Computer Engineering & Information Technology*, vol. 5, no. 8, pp. 66-70, 2009.
[21] T. Y. Chen, T. H. (C. H.) Chen, D. J. Wang, and Y. C. Chiou, Real-time video object segmentation algorithm based on change detection and background updating, *International Journal of Innovative Computing, Information and Control*, vol. 5, no. 7, pp. 1797-1810, 2009.
[22] G. Cao, Y. Zhao and R. Ni, Edge-based blur metric for tamper detection, *Journal of Information Hiding and Multimedia Signal Processing*, vo1. 1, no. 1, pp. 20-27, Jan. 2010.